PPPL-2063

PPPL-2063

PPPL--2063

DE84 006279

ION TRANSPORT STUDIES ON THE PLT TOKAMAK DURING NEUTRAL BEAM INJECTION

By

S. Suckewer, A. Cavallo, S. Cohen, C. Daughney, B. Denne, E. Hinnov, J. Hosea, R. Hulse, D. Hwang, G. Schilling, B. Stratton and R. Wilson

DECEMBER 1983

PLASMA PHYSICS LABORATORY

PRINCETON UNIVERSITY

PRINCETON, NEW JERSEY

PREPARED FOR THE U.S. DEPARTMENT OF ENERGY, UNDER CONTRACT DE-AC02-76-CHO-3073.

ION TRANSPORT STUDIES

ON THE PLT TOKAMAK DURING NEUTRAL BEAM INJECTION

S. Suckewer, A. Cavallo, S. Cohen, C. Daughney, B. Denne[+], E. Hinnov,

J. Hosea, R. Hulse, D. Hwang, G. Schilling, B. Stratton[++],

and R. Wilson

Princeton University, Plasma Physics Laboratory

Princeton, New Jersey 08544

[+]Stipendiary of the Swedish Natural Science Research Council

[++]Johns Hopkins University, Department of Physics

Baltimore, Maryland 21218

ABSTRACT

Radial transport of ions during co- and counter-neutral beam heating in the PLT tokamak has been studied, using molybdenum and scandium ions as tracer elements. The time evolution of the radial profiles of several ionization stages of both elements, injected by laser blowoff during the neutral beam heating, were measured under three significantly different beam-plasma combinations. No noticeable differences in the radial profiles attributable to the beam direction were observed. However, a given injected amount resulted in considerably larger interior concentrations of the tracer element in the counter-beam heating cases, suggesting larger penetration of the plasma periphery. Computer simulation with the MIST code suggests a net inward drift of the order 10^3 cm/sec superposed to a diffusion coefficient of the order 10^4 cm^2/sec for both scandium and molybdenum ions. Injection of larger amounts of the tracer element, sufficient to cause measurable central electron

temperature changes, resulted in dramatic changes in ion-state distributions, making some appear peaked in the center while others disappeared. This effect could be produced with both co- and counter-beam heating, but with lesser amounts in the latter case. It is interpreted as rearrangement of the ionization balance, rather than any preferential accumulation of the injected element.

I. INTRODUCTION

In earlier experiments [1] on the PLT tokamak with high power, neutral beam heating some significant differences were observed to arise from the beam direction relative to the plasma current at comparable beam powers. In particular, the level of radiation by ions of impurity elements originating from vacuum vessel walls or limiters was considerably higher in the case of counter-injection than with co-injection or even with simultaneous co- and counter-injection. The latter statement implies that the difference is not due to sputtering by prompt beam particles, but to a change in plasma characteristics.

This observation has been invoked at times to support a radial ion transport model [2,3] in which the beam-induced toroidal rotation produces an inward drift and central accumulation of heavy, highly charged impurity ions in the case of counter-injection, and an outward drift and expulsion in the case of co-injection. Some experimental observations on the ISX-B tokamak [4] involving light-intensity measurements of ions of deliberately injected elements have been interpreted as direct confirmation of such an ion transport mechanism in tokamaks. However, in the above-mentioned PLT experiments [1], there is nothing that would suggest substantially different ion confinement

properties between co- and counter-injection cases. There is only a larger impurity concentration in the latter case that is correlated with a higher peripheral temperature. It is surmised that the higher edge temperature increases the sputtering rate and hence the impurity concentration.

In order to elucidate the ion transport and confinement properties of the beam-heated plasmas, we have undertaken a detailed and systematic study of the ion dynamics. Two different elements, scandium and molybdenum, were injected into beam-heated discharges, and the behavior in time and space for a number of different ionization stages of both elements were measured, both for co-injection and counter-injection, for three different beam-plasma combinations, and various beam-power levels and toroidal field strengths. The experiments thus compare the behavior of two significantly different elements in the same plasma, and the effect of changing beam-direction on both.

The experimental results are compared with modeling calculations by the MIST code [5], which uses experimental electron temperature and density profiles, theoretical or empirical ionization and recombination rates, and adjustable radial transport rates, with the results subject to the multiple constraints of all the observed ionization stages. These constraints consist not only of the time and space variations of the observed emissivities, but also of the absolute ion densities relative to the carefully monitored quantities of the injected elements.

Before discussing the results of the measurements we shall give an overview of the somewhat complicated experimental setup and of the background information required for the acquisition and quantitative interpretation of the data.

II. EXPERIMENTAL ARRANGEMENT

The geometry of the experiment and the toroidal location of the various diagnostics are shown in Fig. 1. The electron temperature and density profiles were determined from the TV Thomson scattering (TVTS) measurements, and their time variation from the multichannel electron cyclotron second harmonic emission (ECE) and the microwave interferometer, respectively. The total radiated power was monitored with a fast pyroelectric radiation detector, and the short-wavelength (< 400 Å) emission separately with a soft X-ray fluxmeter. The ion temperature profiles were measured from Doppler broadening of various intrinsic and injected impurity ion lines, and separately from neutral hydrogen charge-exchange spectra. The central toroidal plasma rotation was measured from the Doppler shift of the FeXX 2665 Å and TiXVII 3834 Å forbidden lines using the fast rotating mirror system (FARM) [6].

The injected scandium and molybdenum line emissivities were measured with several spectrometers. Some of these measurements were purposely redundant for quantitative intercomparisons. At wavelengths > 2000 Å (Tables I, II) the relative chord brightnesses were repeatedly scanned with the FARM system while the central chord brightness was measured with a separate absolutely calibrated monochromator. In the vacuum UV wavelength range the brightnesses from different chords were measured on a shot-by-shot basis by two different spectrometers. One is a grazing-incidence bichromator (GISMO) with an effective wavelength range of 40-1200 Å, calibrated [7] for absolute intensity measurements <u>in situ</u> by the line branching-ratio method. The other is a 1-meter grazing-incidence multichannel spectrometer (GIMS) which is intensity calibrated against synchrotron radiation from the SURF II facility at the

National Bureau of Standards [8]. The radial scanning range of the grazing-incidence spectrometers is somewhat limited, to about r ~20 cm for GISMO and r ≤ 22 cm for GIMS. This was adequate for most of the vacuum UV lines of interest, but for some cases as noted below, only the time behavior and total brightness could be determined without the radial distribution. The measured chord brightnesses were then Abel-inverted to yield the local emissivity of the line, and the latter converted to the corresponding ion density as described below.

III. PRELIMINARY INVESTIGATIONS

A considerable amount of background information has been necessary to acquire and interpret the experimental data discussed below.

First, there is the question of the most suitable elements for the transport study. The ion mass is an important parameter in many possible cross-field transport mechanisms, including in particular the rotation-induced transport models [2,3]. Hence, at least two elements with significantly different masses should be considered. Moreover, ions of each element in the various ionization stage should radiate in the plasma region of principal interest. Lines should be free from substantial interference from other lines of the same element (e.g., strong higher-order lines from earlier states of ionization) and also from strong lines of intrinsic impurities in the plasma (e.g., oxygen and carbon resonance lines). Furthermore, it is important to be able to observe several adjacent ionization states in order to provide the necessary constraints on interpretation of the data. Comparison of two different elements should also enable an evaluation, to some extent, of the

effect of uncertainty in ionization and recombination rate coefficients on transport analysis. Scandinum (Z = 21, mass M ≈ 45) and molybdenum (Z = 42, M ≈ 96) were chosen to fulfill these multiple criteria. The appropriate transitions and wavelengths for these elements have been determined in earlier studies [9-11].

The spectral lines actually used in the present experiments are listed and described in Tables I and II. The ionization potentials (in keV) in the last column indicate the approximate electron temperatures at which these ions are (radially) located in the plasma. The excitation potentials of all the transitions under consideration are much smaller than the ionization potentials with the consequence that the emissivities are practically independent of temperature. The radiative transition rates (in sec^{-1}) do not generally determine the brightness of the line (which is given by appropriate collisional excitation rates), but they are of interest in estimating their density dependence. At the plasma densities under consideration ($\sim 3 \times 10^{13}$ cm^{-3}) the emissivities vary linearly with electron densities for $A > 10^5$ sec^{-1} and are expected to be practically independent of densities when $A < 10^3$ sec^{-1}. The radiative rates for many of these transitions have been calculated recently [12-15], others in the tables have been estimated with an accuracy adequate for the present purposes. The specific emissivity, ε_λ, i.e., the rate of photon emission per ion, is the product of the collisional excitation rate and the electron density for the E1 lines. For the M1 lines, ε_λ requires a detailed collisional-radiative evaluation, which generally involves considerable uncertainties. This has been systematically calculated recently [16] for the n = 2 shell of several elements including scandium. For the more complicated molybdenum ions we have made empirical determinations [17], which are still in rather preliminary stages of development. Thus, accurate evaluations of all the relevant ion densities are not yet feasible,

and in the present paper we discuss mostly the relative variations, with only some allusions to absolute values.

The second aspect of the preliminary experiments concerns the injection of the tracer element. The laser blowoff method [18] of introducing metallic elements into plasmas has been used for some time. But there remains the question of the reproducibility of the injection mechanism, i.e., the relationship between the amount ablated, the amount reaching the edge plasma, and the amount reaching the interior of the plasma. Also, the effects of the injected material on the plasma properties [19,20] must be considered.

In the principal part of the experiment the injected amount of scandium or molybdenum was kept sufficiently low to avoid measurable changes in the electron temperature and other plasma properties. Some of the effects of larger injected amounts, resulting in noticeable temperature changes are also described.

IV. EXPERIMENTAL RESULTS

Three different sets of experimental conditions were investigated:

1) A single H° beam, in either the co- or counter-direction, was fired into an ohmically heated D^+ plasma with a line average electron density $\bar{n}_e \sim 4 \times 10^{13} cm^{-3}$, toroidal field $B_\phi = 32$ kG, and plasma current $I_p \simeq 480$ kA. The beam power was about $P_{NB} \simeq 0.5$ MW, i.e., comparable to the ohmic input power, and the beam was applied for 150 ms at 450 ms after the start of the discharge;

2) An ohmically heated D^+ plasma similar to above ($I_p \simeq 500$ kA, $\bar{n}_e \simeq 3 \times 10^{13} cm^{-3}$, $B_\phi = 31$ kG) was used as the target for two H° beams in either the

co- or counter-direction, i.e., the conditions were similar to those in (1) except that a beam power $P_{NB} \simeq 0.9$ MW was used. In this case, the co- to counter-change was made by reversing the direction of B_ϕ and I_p while using the two beams which are pointed in the same toroidal direction (see Fig. 1);

3) In order to increase the expected [2,3] beam-direction effect, the toroidal field was lowered to $B_\phi = 16$ kG, and the two beams were used with D^0 at the highest available power of $P_{NB} = 1.0$ MW, fired into an H^+ plasma for the largest toroidal rotation. The target plasma current was $I_p \simeq 430$ kA, and the electron density $\bar{n}_e \simeq 2.5 \times 10^{13} cm^{-3}$.

In all cases the aperture limiter was a graphite rail at a = 40 cm. The scandium or molybdenum injection occurred 50 msec after the start of the beam heating, at which time the plasma had reached a quasi-steady-state.

We shall now describe some aspects of each of these conditions with emphasis on comparing the effect of the beam direction on the behavior of the injected ions.

Figures 2 and 3 show, respectively, the time behavior of the central chord brightness (representative of the number of corresponding ions along the line-of-sight) for four ionization states of scandium, and the radial profiles of five states, normalized to their maxima. Also shown are the electron temperature and density profiles, which did not vary measurably as a result of the scandium injection. Under these conditions the shapes of the radial ion profiles remain remarkably constant, and the absolute values increase and decrease according to the intensity variation in Fig. 2.

There is no significant difference in either the time or the space dependence of the emission from these ions attributable to the beam direction. At most there is a suggestion of slightly faster radial motion in the counter-injection case resulting in broader profiles at intermediate radii.

The same conclusion was reached from observing molybdenum ions, which are not shown for this case for the sake of brevity.

Figures 4, 5, and 6 pertain to the second, two-beam, experimental conditions with a significantly larger beam power, temperature rise, and toroidal rotation resulting from the beam injection.

Figure 4 compares the time behavior of lines from two ions of each element, one nearly central and one more peripheral, as shown in Fig. 5. (The radial location of the ScXI ion, as well as that of ScX in the previous case, could not be measured because of the scan-range limitation of the spectrometers. From indirect evidence they are expected to peak at r ~ 34-36 cm.)

Although the interior ion profiles in the counter-injection case are somewhat sharper, there still is no very significant distinction attributable to the beam direction either in the time behavior or the radial location of ions of either element as well as in the total radiation as indicated by pyroelectric detector measurements. However, a number of comments on these observations are necessary.

First, there is the question of the "sawtooth" oscillations, very evident in the central MoXXXII emissivity in Fig. 4 (also seen with the opposite time behavior in the ScXIX emissivity in Fig. 2). These oscillations are known to be caused by rapid periodic interchange of the plasma, localized about the q = 1 surface [21], i.e., a drop in the interior temperature accompanied by a temporary rise just outside the q = 1 radius (reflected in the rise of the Sc XIX light in Fig. 2), and followed by a slower restoration of the more peaked profile. In the present case, the radial profiles, e.g., of MoXXXII in Fig. 5, are those of the (central) maxima, i.e., just before the onset of each drop. As is evident from Fig. 4 (and Fig. 2), there is also no great distinction in this aspect between co- and counter-injection cases.

Aside from comparison of beam direction, Fig. 5 also compares the behavior of molybdenum ions with scandium. (The different normalization for the two elements is only for clarity.) It is evident that ions of comparable ionization potential (and hence approximately comparable collisional ionization rates) occur nearly at the same radius [i.e., $T_e(r)$]. Persistent uncertainties in the collisional ionization and recombination rates (in addition to the unknown transport rate) still prevent sufficient quantitative analysis of the transport of these ions. It is clear, however, that ions of both elements reach the central part of the discharge in about 20 msec after injection, and disappear with a time constant of about 50 msec, and that the time behavior of ions at the same radius is very similar for both elements.

In principle the local emissivities, shown normalized to their maxima in the figures, may be converted to corresponding ion densities, but for many of the ions, especially in molybdenum, the quantitative correlations are still too uncertain for significantly reliable results. However, in the case of the ns and ns^2 configurations (ScXIX, XVIII, MoXXXII, and XXXI), the conversion is quite reliable, and thus a fairly good estimate of the central density of these elements is available and is discussed in conjunction with the code calculations below.

Although the time and space behavior of the ion distributions is practically independent of the beam direction, there exists a significant, reproducible quantitative difference. In order to reach a given central ion density, the amount ablated from the laser target must be reduced by a factor between 2 and 3 in the counter-injection case, compared to the amount required for co-injection, or alternatively, with a given ablated amount the resultant ion density in the counter-injection case is 2-3 times larger. The reason for this difference is not unequivocably known, but it is probably connected with

peripheral plasma conditions, and is probably also the cause of the observed co-counter difference in Ref. [1].

However, the radial temperature and electron density profiles in Fig. 6 are remarkably similar. Although the difficult to measure near-peripheral conditions could not be investigated in detail due to lack of time, there is no evidence of the substantial edge temperature difference of the earlier measurements [1] in the present data. The reason for this could be in different gas inlet handling (higher n_e at plasma edge during counter-injection) or vacuum vessel and limiter conditioning. Nevertheless, the difference in the injected ion penetration persists in the present condition.

Figure 7 shows a sample of the molybdenum ion density profiles computed with the one-dimensional MIST code [5] for the experimental $T_e(r)$ and $n_e(r)$ profiles shown in Fig. 6 and a very simple set of assumed ion transport terms: a radially constant diffusion coefficient, D, an inward directed radial velocity with r/a radial dependence, and a recycling coefficient $\rho = 0.5$. These coefficients reproduce fairly well the observed central density (from the known starting amount) and the time behavior of the various ionization stages. The correspondence with observed radial profiles is fair, but with significant discrepancies at larger radii. Variation of the transport coefficients indicates that:

a) An inward convective velocity of roughly the order of magnitude shown is needed in addition to the diffusion flux. (The linear r-dependence is not necessarily appropriate.) The central density, from a given initial injected amount, depends sensitively on this velocity and on the recycling coefficient ρ. The specific values taken for V and ρ have yielded a viable model, but should not be taken as quantitatively definitive. This is particularly true for the recycling coefficient, ρ.

b) The diffusion coefficient is probably right within about a factor of 2, but might also have some radial dependence.

c) These transport coefficients are not very different from the particle transport required to produce observed ion temperatures and energy replacement times in ohmic heating discharges.

A recent study of heavy ion transport in the TFR tokamak [22] has reached rather similar conclusions, both on the necessity of the net inward drift, and the general magnitude of the coefficients.

In the third experiment with the lower toroidal field (and lower plasma current), the electron temperatures were noticeably lower, as expected. [See $T_e(r)$ profiles in Fig. 8 for the Mo injection case; in the case of Sc injection the $T_e(r)$ profiles were practically the same.] As a consequence, MoXXVII (and Sc XIX) was found to be the terminal state, i.e., higher states of ionization were not produced in the discharge. It is of interest to note that the MIST code, given the new temperature profile, reproduced this result remarkably well with the same transport rate coefficients as given in Fig. 7.

The comparison of co- and counter-injection results of the time behavior and radial profiles of several molybdenum and scandium ions are shown in Figs. 8 – 9, and 10-11, respectively. The large fluctuations in the MoXXVII ion brightness in Fig. 9 are again caused by the sawtooth oscillations, and this is also evidently the cause of some of the irregularities in the intensities of other interior ions, such as ScXVIII and MoXXIII. There is a notable up-down asymmetry in the emissivity profiles around 20-30 cm which is enhanced by the superimposed fast decay time of the line intensities during the fast radial scans. The real up-down asymmetry near $r \sim 30$ cm is represented by profiles of the intrinsic CV emissivity, which remains approximately constant in the time scale of the radial scan. In general, the relationship of the

behavior of the molybdenum and scandium ions (radial profiles and time evolution) to each other and to the temperature profile is qualitatively the same as in the previous experiments. In particular, the absence of any general difference in the time and space variations that could be ascribed to the beam direction is very obvious.

However, the quantitative distinction persists - it took substantially less, 2-3 times, of the injected element to produce a given concentration of interior ions in the counter-injection case than was required in the co-injection case. Possibly the somewhat narrower initial peak of the MoXIII light (Fig. 9) , perhaps also discernible in ScXIII (Fig. 11), indicates a more rapid penetration of the peripheral plasma by the injected element ions in the counter-injection case. However, peripheral ions with localized sources can exhibit toroidal, as well as poloidal and radial variations, so the global interpretation of their emissivity must be done with circumspection.

V. INJECTION OF PERTURBING AMOUNTS OF HEAVY ELEMENTS

In the preceding section, the amount of injected molybdenum or scandium was kept so low as to produce no discernible change in the electron temperature profile. Here we shall describe some observations with larger injected amounts of molybdenum.

Clearly, the sudden introduction of a heavy element may perturb the plasma conditions in a number of ways. There is the obvious effect of radiative energy loss, but there is also the introduction of cold electrons and a change of the effective ionic charge (Z_{eff}), all of which tend to alter

the radial current distribution and hence may produce cumulative changes in particle transport and lead to disruption. However, if a disruption is not produced immediately (i.e., within 10-20 msec), the preinjection plasma conditions are generally restored within a few energy-replacement times, i.e., 100-200 msec in typical PLT discharges. There are some exceptions to this behavior, perturbations that last for a much longer time, but these phenomena are not yet adequately understood.

In general, it is much easier to produce noticeable perturbations to the plasma with heavier injected elements than with lighter ones and, as the preceding section might imply, it is easier to perturb a counter-beam heated discharge than a co-beam heated one. Figure 12(a) shows the observed time behavior of the emission of three molybdenum ions, and the central electron temperature (from ECE measurements) resulting from injection of about 10^{17} Mo atoms into a counter-heated discharge, described under experimental condition (2) above. This is the same amount, and the same discharge that produced with co-injection the solid curves in Fig. 4(b). The dashed curves in Fig. 4(b) were observed as a result of injecting about 4×10^{16} Mo atoms (this reduction produced about the same intensity of both MoXXXII and MoXXIII light as the co-injection case).

Figure 12(b) shows the radial profiles of the MoXXIII 3553 Å line obtained with the fast rotating mirror system near the indicated times. Although the profiles are rather lopsided, partly because of the rapid time-variation of the distribution, there is no doubt that the MoXXIII ion becomes centrally peaked as its intensity peaks in time, while the higher ionization states disappear.

A comment on the apparent residual intensity of the MoXXXII line is necessary, considering that the MoXXX intensity almost disappears. What is

actually shown is the signal of the two channels of the GISMO bichromator at the indicated wavelengths. This signal includes pseudocontinuum background radiation mostly from light scattered on the grating. This background light is much stronger near the lower-wavelength setting, and while it is normally small compared to the strong 177 Å resonance line, it is probably much enhanced during the peak of the perturbation, about 470-520 msec. Not enough machine time was devoted to this part of the experiment to ascertain this experimentally. However, in our opinion the 177 Å signal during this interval is mostly background light, although at later times, with increasing temperature and decreasing perturbation intensity, it is again mostly MoXXXII light, consistent with the MoXXX signal.

The MIST code at present does not allow time variations of temperature profiles, but an approximate idea of the magnitude of the variation of the ion profiles with changes in temperature may be obtained by comparing steady-state solutions corresponding to temperatures before injection and during the minimum, i.e., at 450 and 480 msec. The results for the MoXXIII and MoXXX ions are given in Fig. 13 for the same total amount of molybdenum. Although the calculated MoXXIII profile after the temperature drop is distinctly too broad, the general magnitude for both ions are in quite good agreement with the observations. Thus, it appears probable that the observed emission effects in Fig. 12 are produced largely, and perhaps entirely by self-consistent readjustment of the ionization rates to the changing temperature profile, without substantial changes in the molybdenum concentration or transport. Yet, if one only had the MoXXIII behavior in Fig. 12 (and the corresponding co-injection case, with the same injected amount, in Fig. 4), and especially if the former led to disruption, then it might appear that the counter-injection heating led to a rapid preferential accumulation of molybdenum in the center.

Qualitatively, the same effect may be produced in plasmas with co-injection heating, as shown in Fig. 14 - it just requires more molybdenum. And of course other elements could be used equally well, with the general provision that the lighter the element, the larger must be the injected amount for a given perturbation.

VI. CONCLUSIONS

We have found no evidence of qualitative differences of heavy ion transport in the PLT tokamak discharges attributable to the direction of the heating neutral beam. In both co- and counter-heated plasmas, and with different beam and target-plasma combinations, the time and space behaviors of injected molybdenum and scandium ions were remarkably similar.

Nevertheless, there is a substantial quantitative distinction between the co- and counter-beam heated plasmas. With a given amount of injected element, the ion densities that reach the interior of the plasma are 2-3 times larger in the counter-heated case, with the corollary that the counter-heated plasma is more easily perturbed by a given amount of the injected element. The reason for this difference is not known, but it must have to do with peripheral plasma conditions. This behavior is consistent with our earlier [1] observations, that counter-heated plasmas contained more wall and limiter materials, and hence emitted more radiation.

When the amount of injected tracer element is sufficient to affect significantly the electron temperature profile, the observed effects can very convincingly mimic changes in transport properties, and particularly accumulation of heavy ions in the center of the plasma. In view of the preceding paragraph, this behavior can easily be attributed to counter-beam heating alone.

Transport modeling with the MIST code can very successfully reproduce the gross features of the observed ion behavior with a very simple set of transport coefficients: a diffusion coefficient of the order 10^4 cm^2/sec together with an inward drift velocity of the order of 10^3 cm/sec. These are preliminary results, as there are significant problems of detail that will require careful empirical study under optimized experimental conditions. It is, however, clear that transport coefficients of this magnitude are required to reproduce the observed behavior of injected ions in these discharges.

Further improvements of ionization and recombination (particularly including charge-exchange recombination) rates of ions in other than the simplest electron configuration, as well as quantitative evaluation of specific emissivities of the transitions of the type employed in this paper are essential for more adequate confinement studies, as well as other high-temperature diagnostics.

ACKNOWLEDGMENTS

The authors wish to express their gratitude to H. Furth for encouragement and support, and to K. Burrell (G.A.), J. Hogan and D. Sigmar (ORNL) for very helpful discussions. Our experiments would be impossible without excellent work by the PLT Operating Team, particularly P. Colestock, F. Jobes, E. Meservey, and J. Strachan, the Neutral Beam Team, Surface Physics Group, and the Technical Crew led by W. Mycock. B. Denne is grateful to the Swedish Natural Science Research Council (NFR) for a scholarship grant that has allowed her to participate in these experiments.

This work was supported by US DOE Contract No. DE-AC02-76-CHO-3073.

REFERENCES

[1] SUCKEWER, S., HINNOV, E., HWANG, D., SCHIVELL, J. SCHMIDT, G.L. et al., Nucl. Fusion 21 (1981) 981.

[2] STACEY, W.M., SIGMAR, D.J., Nucl. Fusion 19 (1979) 1665.

[3] BURRELL, K.H., OHKAWA, T., WONG, S.K., Phys. Rev. Lett. 47 (1981) 511.

[4] ISLER, R.C., MURRAY, L.E., KASAI, S., ARNURIUS, D.E., BATES, S.C., et al., Phys. Rev. Lett. 47 (1981) 643.

[5] HULSE, R.A., Nucl. Technol./Fusion 3 (1983) 259.

[6] SUCKEWER, S., EUBANK, H.P., GOLDSTON, R.J., HINNOV, E., SAUTHOFF, N., Phys. Rev. Lett. 43 (1979) 207.

[7] HINNOV, E., in Diagnostics for Fusion Experiments, E. Sindoni and C. Wharton, Eds., Pergamon Press, Oxford, England, (1979) 139.

[8] HODGE, W.L., STRATTON, B.C., MOOS, H.W., Rev. Sci. Instrum. (1983), to be published.

[9] SUCKEWER, S., CECCHI, J., COHEN, S., FONCK, R., HINNOV, E., Phys. Lett. 80A (1980) 259.

[10] SUCKEWER, S., HINNOV, E., COHEN, S., FINKENTHAL, M., SATO, K., Phys. Rev. A26 (1982) 1161.

[11] HINNOV, E., SUCKEWER, S., COHEN, S., SATO, K., Phys. Rev. 25A (1982) 2293.

[12] CHENG, K.T., KIM, Y.K., DESCLAUX, J.P., At. Data Nucl. Data Tables 24, 111 (1979).

[13] HUANG, K.N., KIM, Y.K., CHENG, K.T., At. Data Nucl. Data Tables 28 (1983) 355.

[14] KAUFMAN, V. and SUGAR, J., Bull. Am. Phys. Soc. 28 (1983) 921.

[15] BIEMONT, E. and BROMAGE, G.E., M.N. Roy. Astr. Soc. (1983) to be published.

[16] FELDMAN, U., DOSCHEK, G.A. BHATIA, A.K., J. Appl. Phys. 53 (1982) 8554.

[17] HINNOV, E. DENNE, B., HULSE, R., SUCKEWER, S., Bull. Am. Phys. Soc. 28 (1983) 922.

[18] MARMAR, E., CECCHI, J., COHEN, S., Rev. Sci. Instrum. 46 (1975) 1149.

[19] MANOS, D., RUZIC, D., MOORE, R., COHEN, S., J. Vac. Sci. Technol. 20 (1982).

[20] COHEN, S., CECCHI, J., DAUGHNEY, C., DAVIS, S., DIMOCK, D., et al. J. Vac. Sci. Technol. 20 (1982) 1226.

[21] HINNOV, E., SUCKEWER, S., et al. Bull. Am. Phys. Soc. 25 (1980) 902.

[22] EQUIPE TFR, Nucl. Fusion 23 (1983) 550.

TABLE I THE WAVELENGTHS AND TRANSITIONS OF SCANDIUM IONS USED FOR EMISSIVITY MEASUREMENTS

Ion	Wavelength (Å)	Transition	Type	$A(sec^{-1})$	ϵ^*_λ	E_i (keV)
ScXIX	326(280)	2s-2p	E1	1.4×10^9	1.3×10^4	1.29
XVIII	180	$2s^2$-2s2p	E1	1.3×10^{10}	5.1×10^4	1.21
	2908	$2s2p(^3P)$	M1	5.1×10^2	18	
XVII	2190	$2s^2 2p(^2P)$	M1	8.5×10^2	500	1.09
	193	$2s^2 2p$-$2s2p^2$	E1	5.6×10^9	1.5×10^4	
XVI	4354	$2s^2 2p^2(^3P)$	M1	2.1×10^2	59	1.0
XIV	3206	$2s^2 2p^4(^3P)$	M1	6.5×10^2	140	0.83
XIII	2637	$2s^2 2p^5(^2P)$	M1	9.7×10^2	325	0.76
XI	505(522)	3s-3p	E1	4.4×10^9	6×10^5	0.25
X	423	$3s^2$-3s3p	E1	1.2×10^{10}	1.1×10^6	0.23

*At electron density $3 \times 10^{13} cm^{-3}$

TABLE II THE WAVELENGTHS AND TRANSITIONS OF MOLYBDENUM IONS USED FOR EMISSIVITY MEASUREMENTS

Ion	Wavelength (Å)	Transition	Type	A(sec^{-1})	$\varepsilon^{*}_{\lambda}$	E_i (keV)
MoXXXII	177(128)	3s-3p	E1	1.6×10^{10}	1.4×10^{4}	1.87
XXXI	116	$3s^2$-3s3p	E1	8.9×10^{10}	6.6×10^{4}	1.81
XXX	490	$3s^2 3p(^2P)$	M1	7.5×10^{4}	4×10^{3}	1.66
XXIX	2841	$3s^2 3p^2(^3P)$	M1	2.9×10^{2}	1.5×10^{2}	1.59
XXVII	570	$3s^2 3p^4(^3P)$	M1	7.9×10^{4}	6×10^{2}	1.43
XXVI	535	$3s^2 3p^5(^2P)$	M1	1.1×10^{5}	1.5×10^{3}	1.37
XXIV	2687	$3p^6 3d(^2D)$	M1	5.5×10^{2}	2.5×10^{2}	1.10
XXIII	3553	$3p^6 3d^2(^3F)$	M1	5.1×10^{2}	1.6×10^{2}	1.03
XVII	4123	$3p^6 3d^8(^3F)$	M1	3.7×10^{2}		0.64
XVI	3708	$3p^6 3d^9(^2D)$	M1	3.2×10^{2}		0.57
XIV	424(374)	4s-4p	E1	8.6×10^{9}	2.0×10^{5}	0.31
XIII	341	$4s^2$-4s4p	E1	2.9×10^{10}	9.3×10^{5}	0.29

*At electron density $3 \times 10^{13} cm^{-3}$

FIGURE CAPTIONS

FIG. 1 Location of plasma diagnostic instruments on the PLT tokamak.

FIG. 2 Time evolution of ScXIII, ScXIX (upper part) and ScX, ScXVIII (lower part) line intensities for co-NBI (solid line) and counter-NBI (dashed line) for $P_{NB} \sim 0.5$ MW, $B_\phi = 32$ kG, and $H^\circ \rightarrow D^+$.

FIG. 3 Radial emissivity profiles of ScXIII-ScXIX for co-NBI (top) and counter-NBI (center). Electron temperature T_e and density n_e profiles are shown at the bottom. Plasma and NB parameters are the same as in Fig. 2.

FIG. 4 Time evolution of (a) ScXI, ScXIX and (b) MoXXIII, MoXXXII line intensities for co-NBI (solid line) and counter-NBI (dashed line) for $P_{NB} \simeq 0.9$ MW, $B_\phi = 31$ kG, and $H^\circ \rightarrow D^+$.

FIG. 5 Radial emissivity profiles of MoXVII-XXXII and ScXIV-XIX for (a) co-NBI and (b) counter-NBI. V_ϕ indicates toroidal (central) plasma rotation. Numbers in parentheses are the ionization potentials of the ions, in keV. Plasma and NB parameters are the same as in Fig. 4.

FIG. 6 T_e, n_e, and T_i profiles for co-NBI (upper part) and for counter-NBI (lower part) for plasma conditions as in Figs. 4 and 5.

FIG. 7 Relative Mo ion density profiles from MIST code modeling (upper part). Measured radial emissivity profiles of various Mo ion lines (from Fig. 5b) normalized to maxima.

FIG. 8 Radial profiles of electron temperature and line emissivities of MoXVI, XVII, XXIII, XXIV, and also the intrinsic CV for co-NBI (upper) and counter-NBI (lower).

FIG. 9 Time evolution of MoXIII, MoXXIII, and MoXXVII line intensities for co-NBI (upper) and counter-NBI (lower).

FIG. 10 Radial emissivity profiles of ScXIII, XIV, XVII, XVIII, and CV for co- (upper) and counter-NBI (lower).

FIG. 11 Time evolution of ScXIII, XVII, and XVIII line intensities for co-NBI (upper) and counter-NBI (lower).

FIG. 12 Time evolution of MoXXIII, XXX, XXXII line intensities and central T_e for large amounts of Mo injected during counter-NBI (upper part) and radial line emissivity profiles (lower part) of MoXXIII for three different times (t_1, t_2, t_3).

FIG. 13 Computer simulation (MIST code) of MoXXIII and MoXXX radial density distributions for conditions as in Fig. 12.

FIG. 14 Time evolution of MoXXIII and MoXXXII line intensities and central T_e for large amounts of Mo injected during co-NBI (upper part) and radial emissivity profiles (lower part) of MoXXIII for three different times (t_1, t_2, t_3).

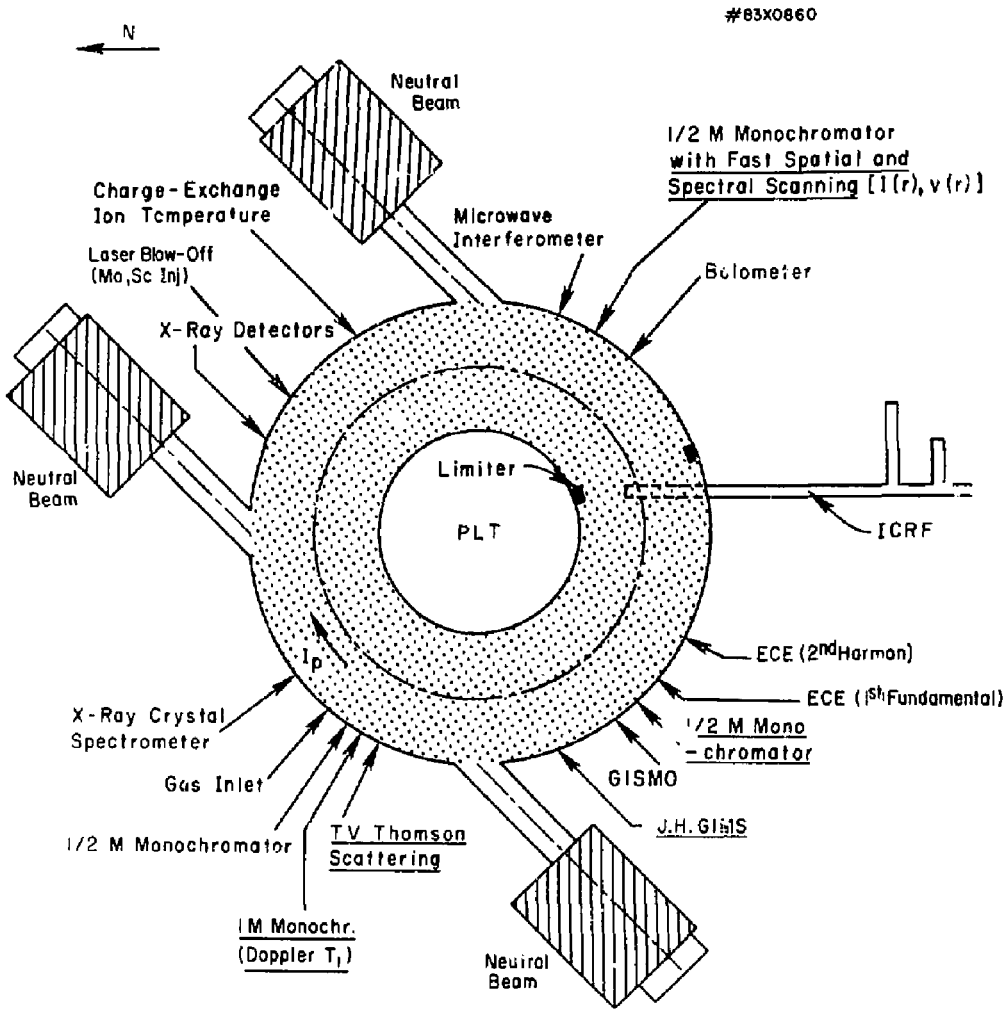
#83X0860
N
Neutral Beam
1/2 M Monochromator with Fast Spatial and Spectral Scanning [I(r), v(r)]
Charge-Exchange Ion Temperature
Microwave Interferometer
Laser Blow-Off (Mo,Sc Inj)
Bolometer
X-Ray Detectors
Neutral Beam
Limiter
PLT
ICRF
I_p
ECE (2nd Harmon)
ECE (1st Fundamental)
X-Ray Crystal Spectrometer
1/2 M Mono -chromator
Gas Inlet
GISMO
J.H. GISMS
1/2 M Monochromator
TV Thomson Scattering
1M Monochr. (Doppler T_i)
Neutral Beam

Fig. 1

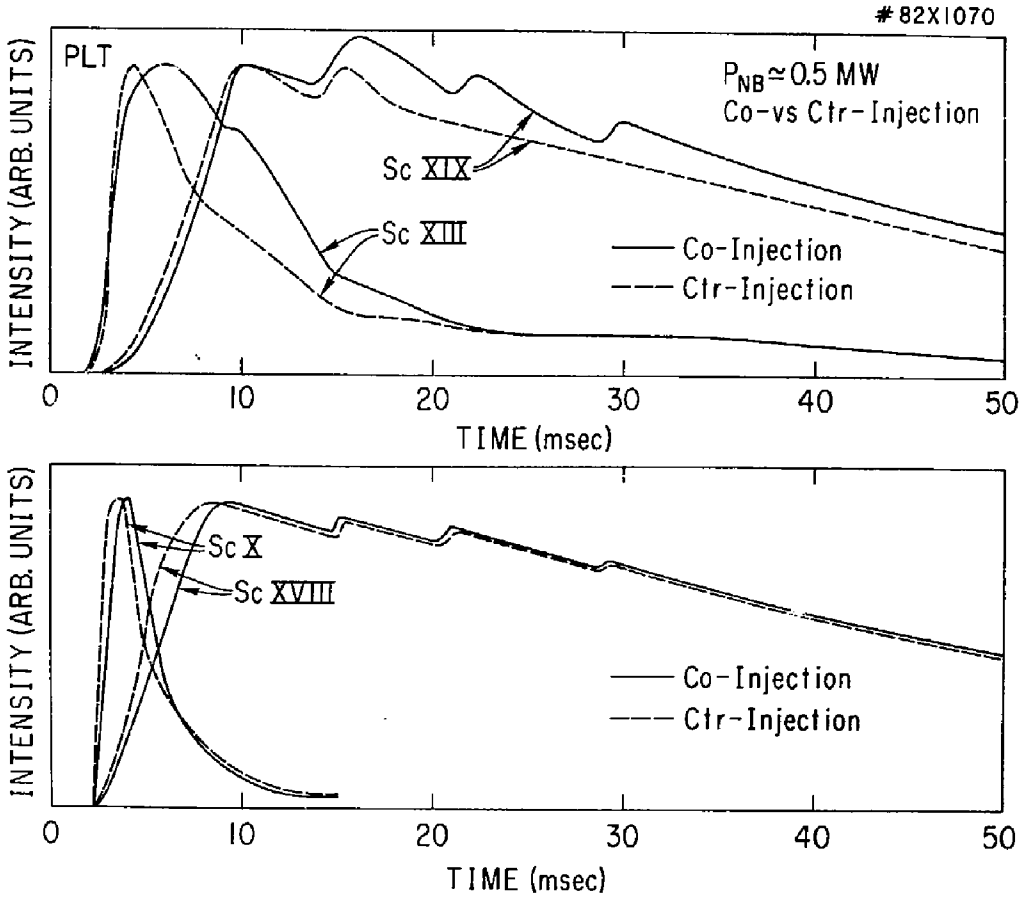
#82X1070
PLT
$P_{NB} \simeq 0.5$ MW
Co-vs Ctr-Injection
Sc XIX
Sc XIII
Co-Injection
Ctr-Injection
INTENSITY (ARB. UNITS)
0
10
20
30
40
50
TIME (msec)
Sc X
Sc XVIII
Co-Injection
Ctr-Injection
INTENSITY (ARB. UNITS)
0
10
20
30
40
50
TIME (msec)

FIG. 2

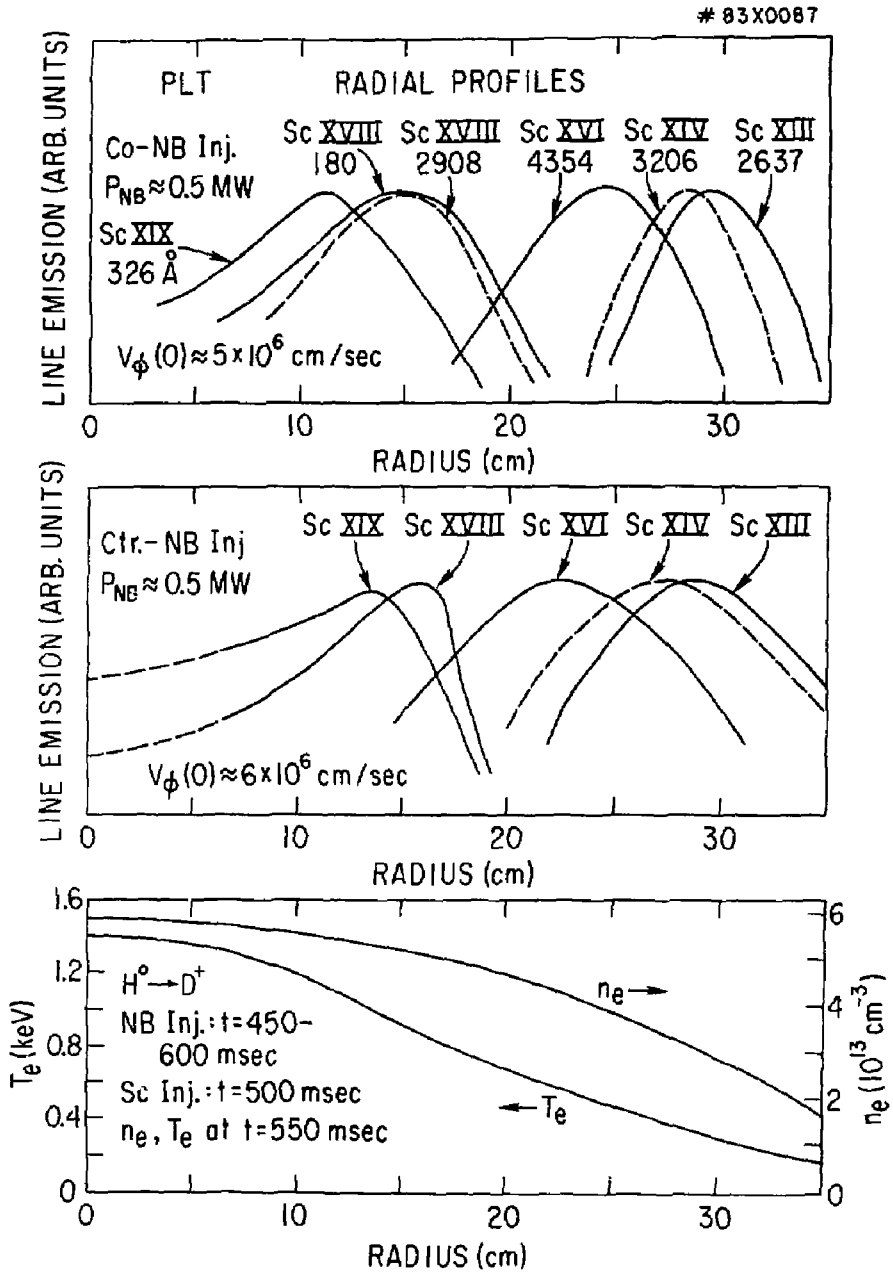
#83X0087
PLT
RADIAL PROFILES
Co-NB Inj.
$P_{NB} \approx 0.5$ MW
Sc XIX
326 Å
Sc XVIII 180
Sc XVIII 2908
Sc XVI 4354
Sc XIV 3206
Sc XIII 2637
$V_\phi(0) \approx 5 \times 10^6$ cm/sec
LINE EMISSION (ARB. UNITS)
RADIUS (cm)
Ctr.-NB Inj
$P_{NB} \approx 0.5$ MW
Sc XIX
Sc XVIII
Sc XVI
Sc XIV
Sc XIII
$V_\phi(0) \approx 6 \times 10^6$ cm/sec
LINE EMISSION (ARB. UNITS)
RADIUS (cm)
$H^0 \rightarrow D^+$
NB Inj.: t=450-600 msec
Sc Inj.: t=500 msec
n_e, T_e at t=550 msec
$n_e \rightarrow$
$\leftarrow T_e$
T_e (keV)
n_e (10^{13} cm^{-3})
RADIUS (cm)

FIG. 3

#83X0655

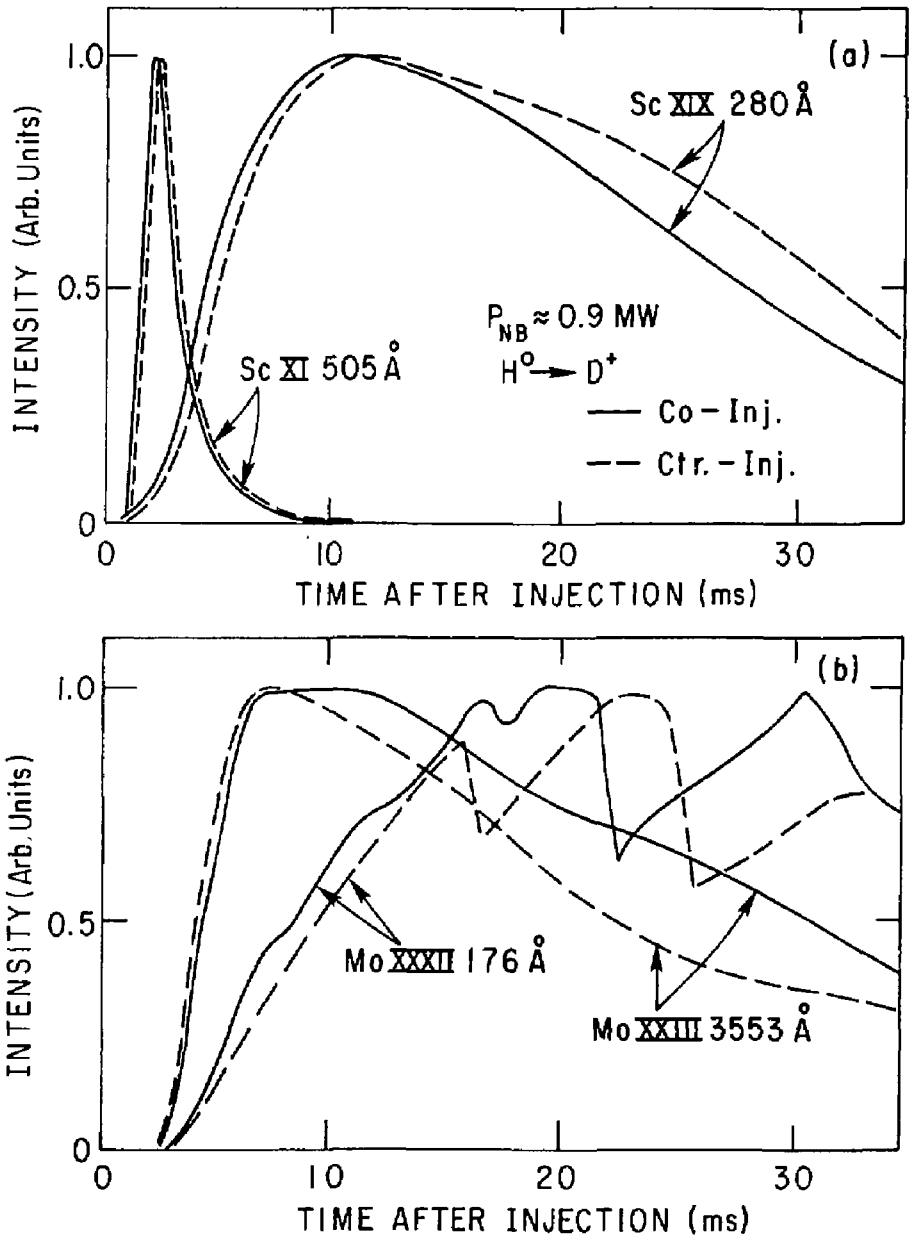

FIG. 4

#83X0069

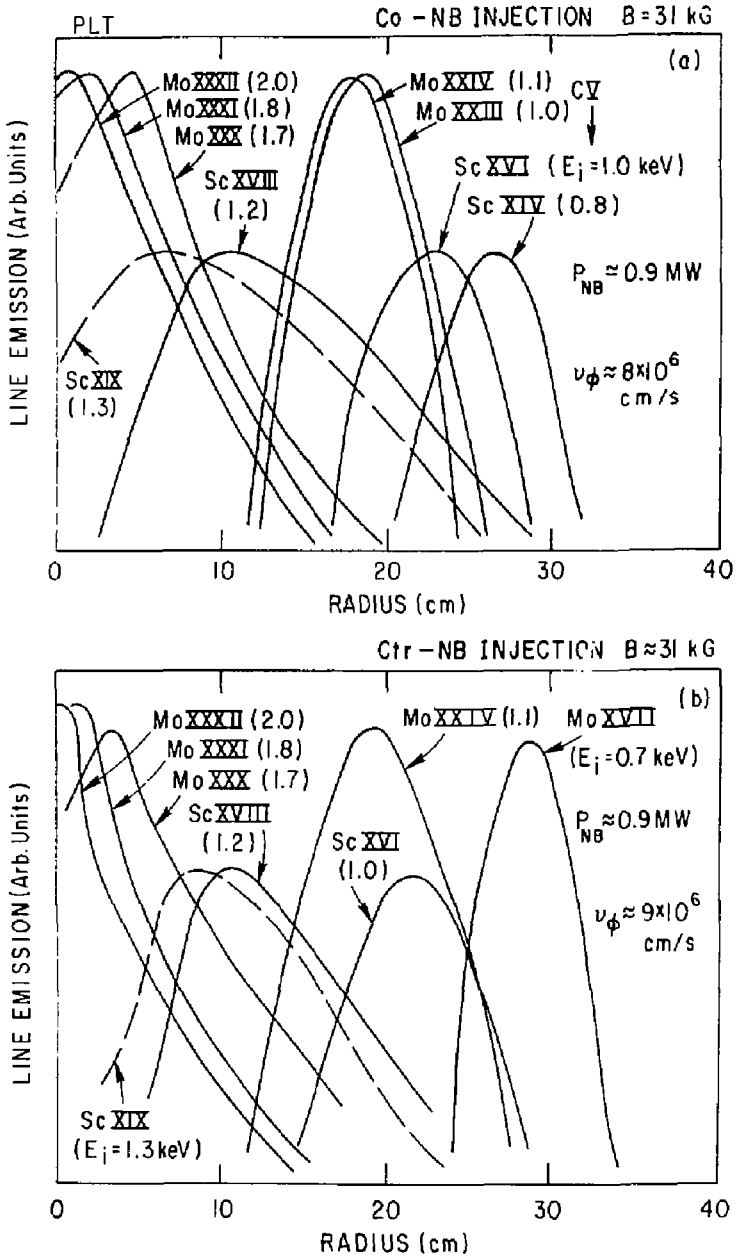

FIG. 5

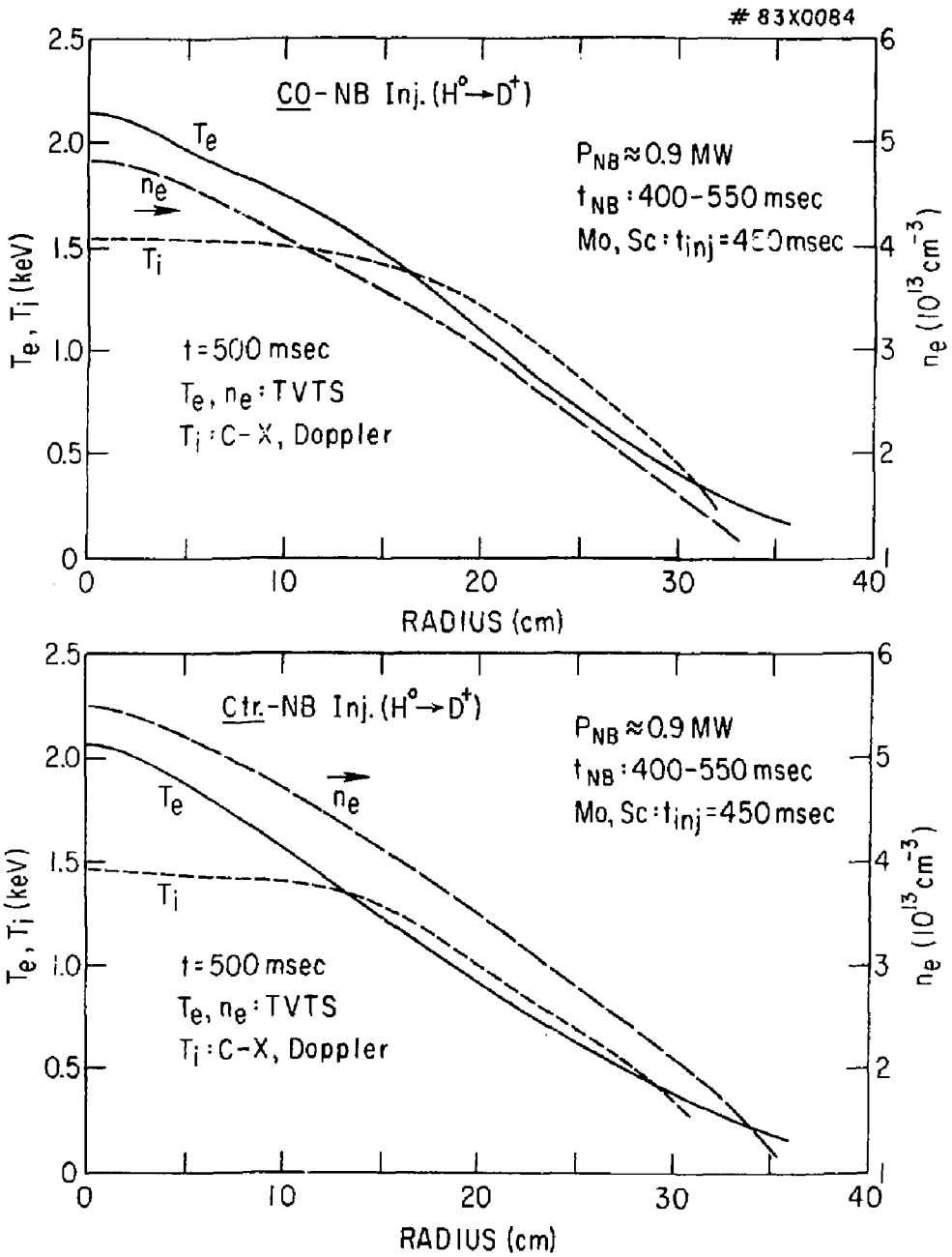
83X0084
CO-NB Inj. ($H^0 \rightarrow D^+$)
T_e
n_e
T_i
$P_{NB} \approx 0.9$ MW
t_{NB} : 400-550 msec
Mo, Sc : t_{inj} = 450 msec
t = 500 msec
T_e, n_e : TVTS
T_i : C-X, Doppler
T_e, T_i (keV)
n_e (10^{13} cm^{-3})
RADIUS (cm)
Ctr.-NB Inj. ($H^0 \rightarrow D^+$)
T_e
n_e
T_i
$P_{NB} \approx 0.9$ MW
t_{NB} : 400-550 msec
Mo, Sc : t_{inj} = 450 msec
t = 500 msec
T_e, n_e : TVTS
T_i : C-X, Doppler
T_e, T_i (keV)
n_e (10^{13} cm^{-3})
RADIUS (cm)

FIG. 6

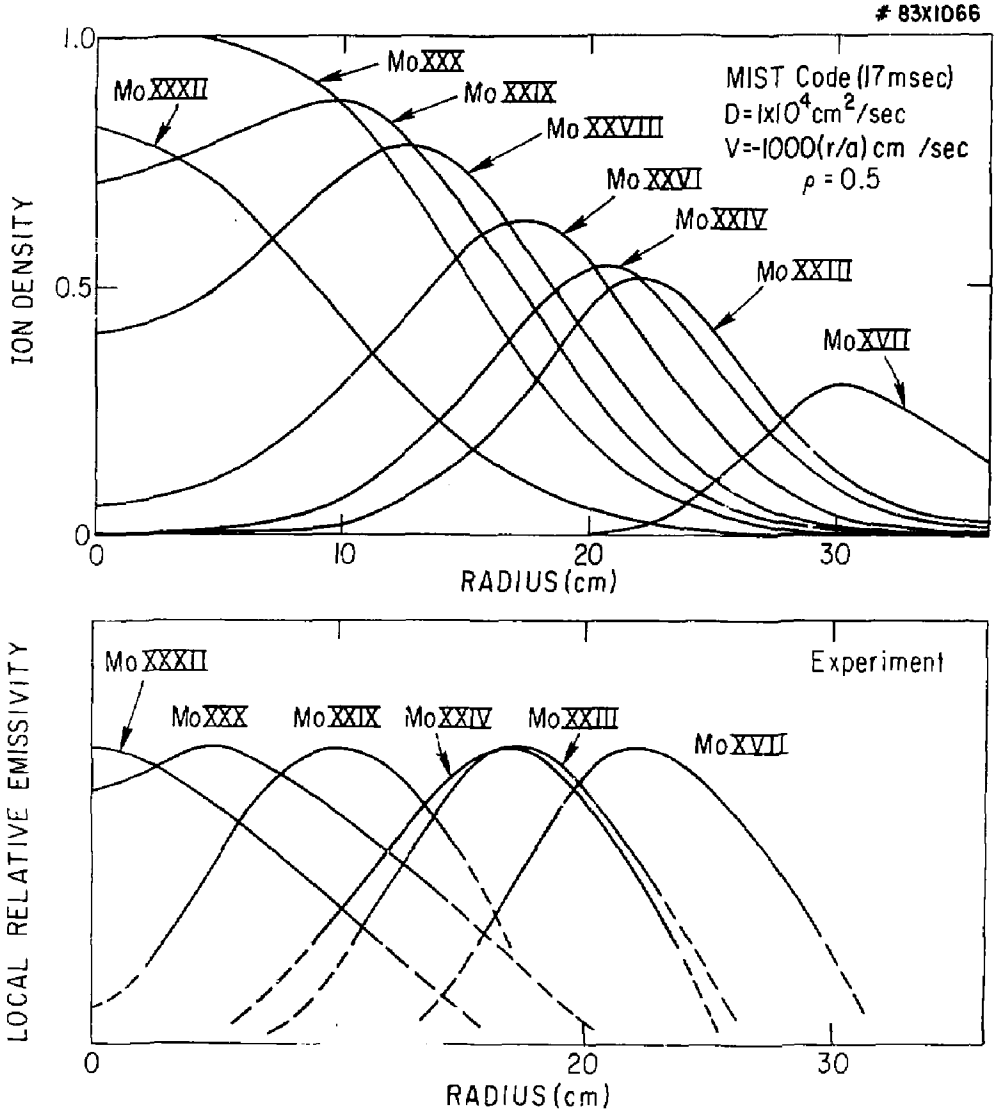
83X1066
1.0
0.5
0
ION DENSITY
Mo XXXII
Mo XXX
Mo XXIX
Mo XXVIII
Mo XXVI
Mo XXIV
Mo XXIII
Mo XVII
MIST Code (17msec)
D=1x10^4 cm^2/sec
V=-1000(r/a) cm /sec
ρ = 0.5
0
10
20
30
RADIUS (cm)
LOCAL RELATIVE EMISSIVITY
Mo XXXII
Mo XXX
Mo XXIX
Mo XXIV
Mo XXIII
Mo XVII
Experiment
0
20
30
RADIUS (cm)

FIG. 7

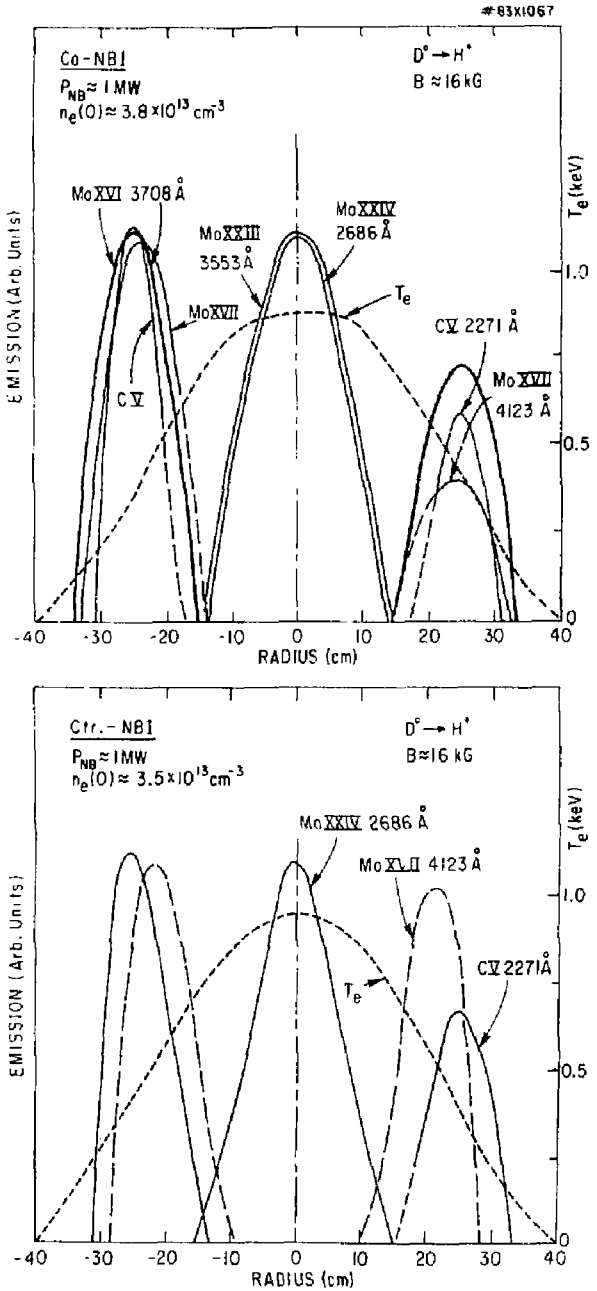
#83x1067
Co-NBI
$P_{NB} \approx 1$ MW
$n_e(0) \approx 3.8 \times 10^{13}$ cm^{-3}
D° → H°
B ≈ 16 kG
Mo XVI 3708 Å
Mo XXIII 3553 Å
Mo XXIV 2686 Å
Mo XVII
T_e
C V
C VI 2271 Å
Mo XVII 4123 Å
EMISSION (Arb. Units)
T_e (keV)
RADIUS (cm)
Ctr.-NBI
$P_{NB} \approx 1$ MW
$n_e(0) \approx 3.5 \times 10^{13}$ cm^{-3}
D° → H°
B ≈ 16 kG
Mo XXIV 2686 Å
Mo XVII 4123 Å
C VI 2271 Å
T_e
EMISSION (Arb. Units)
T_e (keV)
RADIUS (cm)

FIG. 8

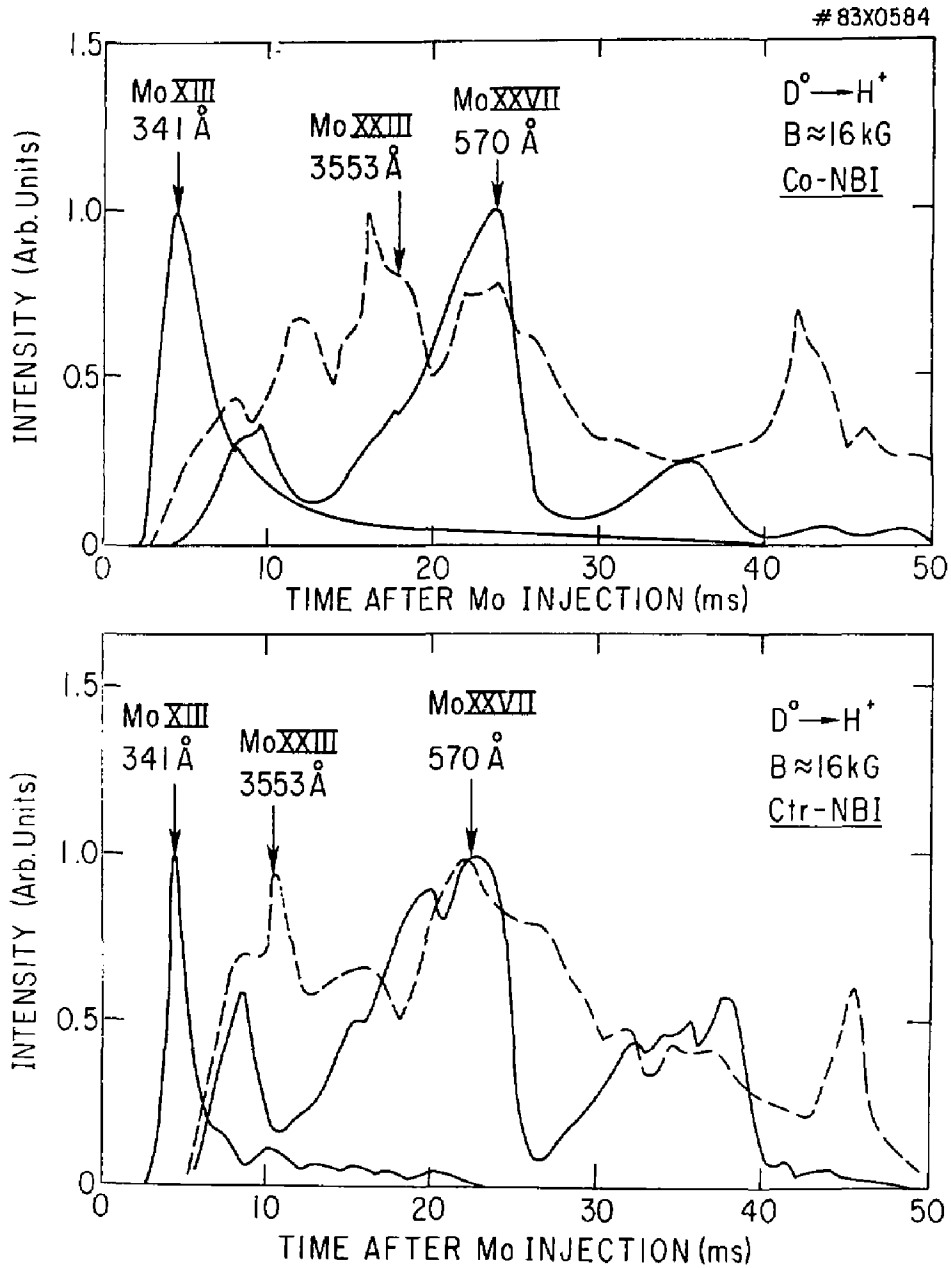
#83X0584
Mo XIII
341 Å
Mo XXIII
3553 Å
Mo XXVII
570 Å
D° → H⁺
B≈16 kG
Co-NBI
INTENSITY (Arb. Units)
TIME AFTER Mo INJECTION (ms)
Mo XIII
341 Å
Mo XXIII
3553 Å
Mo XXVII
570 Å
D° → H⁺
B≈16 kG
Ctr-NBI
INTENSITY (Arb. Units)
TIME AFTER Mo INJECTION (ms)

Fig. 9

#83X0906

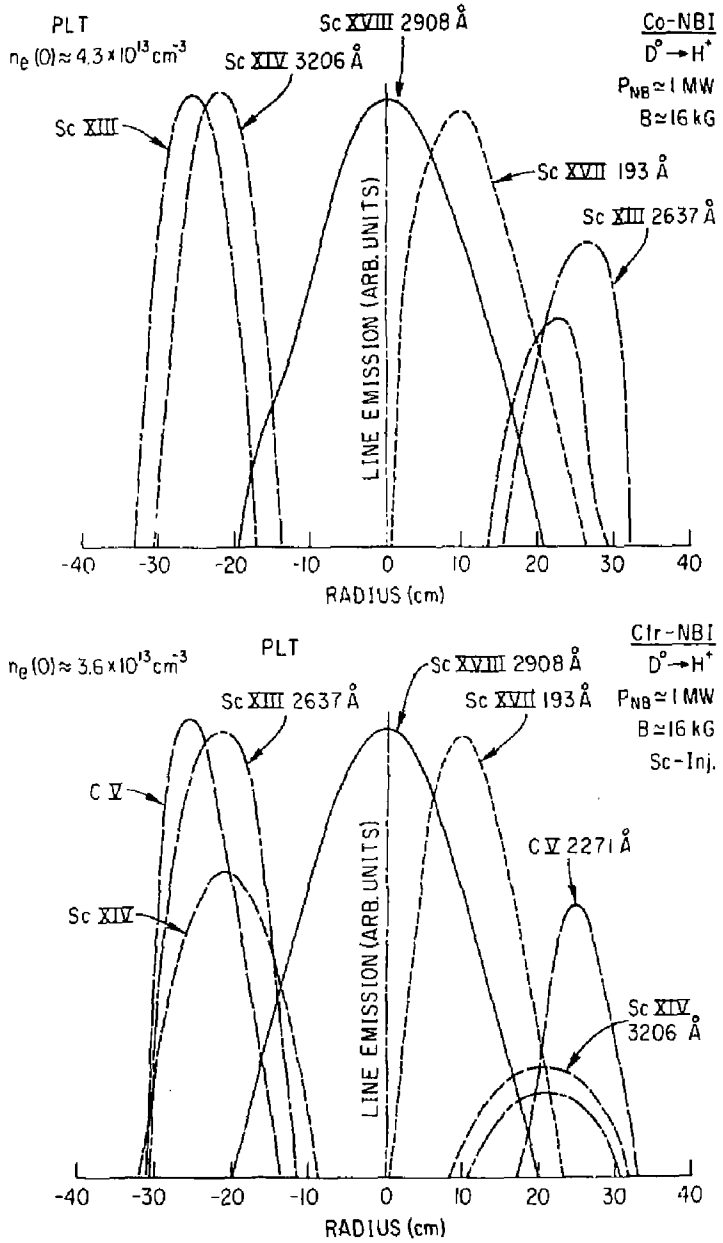

FIG. 10

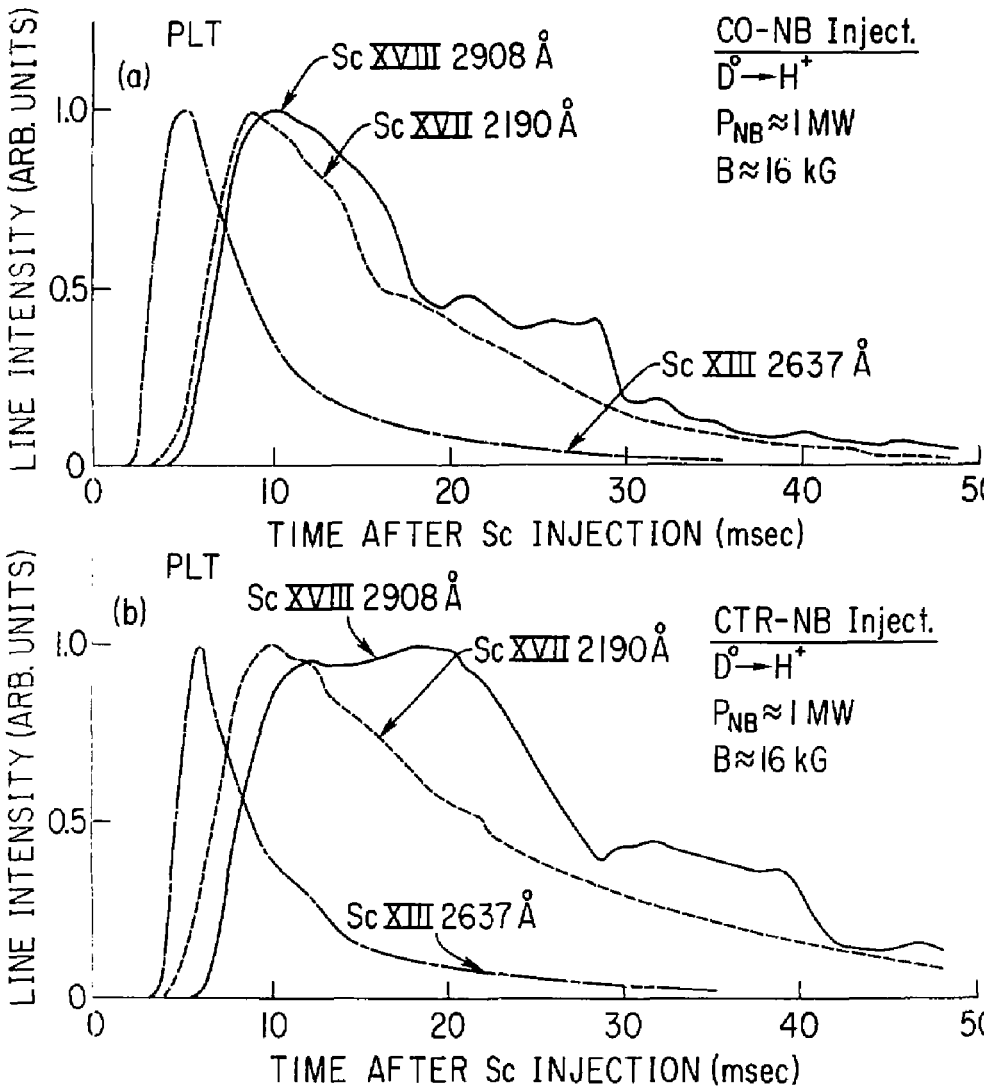
PLT
(a)
Sc XVIII 2908 Å
Sc XVII 2190 Å
Sc XIII 2637 Å
CO-NB Inject.
D°→H⁺
P_NB≈1 MW
B≈16 kG
LINE INTENSITY (ARB. UNITS)
1.0
0.5
0
0
10
20
30
40
50
TIME AFTER Sc INJECTION (msec)
PLT
(b)
Sc XVIII 2908 Å
Sc XVII 2190 Å
Sc XIII 2637 Å
CTR-NB Inject.
D°→H⁺
P_NB≈1 MW
B≈16 kG
LINE INTENSITY (ARB. UNITS)
1.0
0.5
0
0
10
20
30
40
50
TIME AFTER Sc INJECTION (msec)

FIG. 11

83X1064

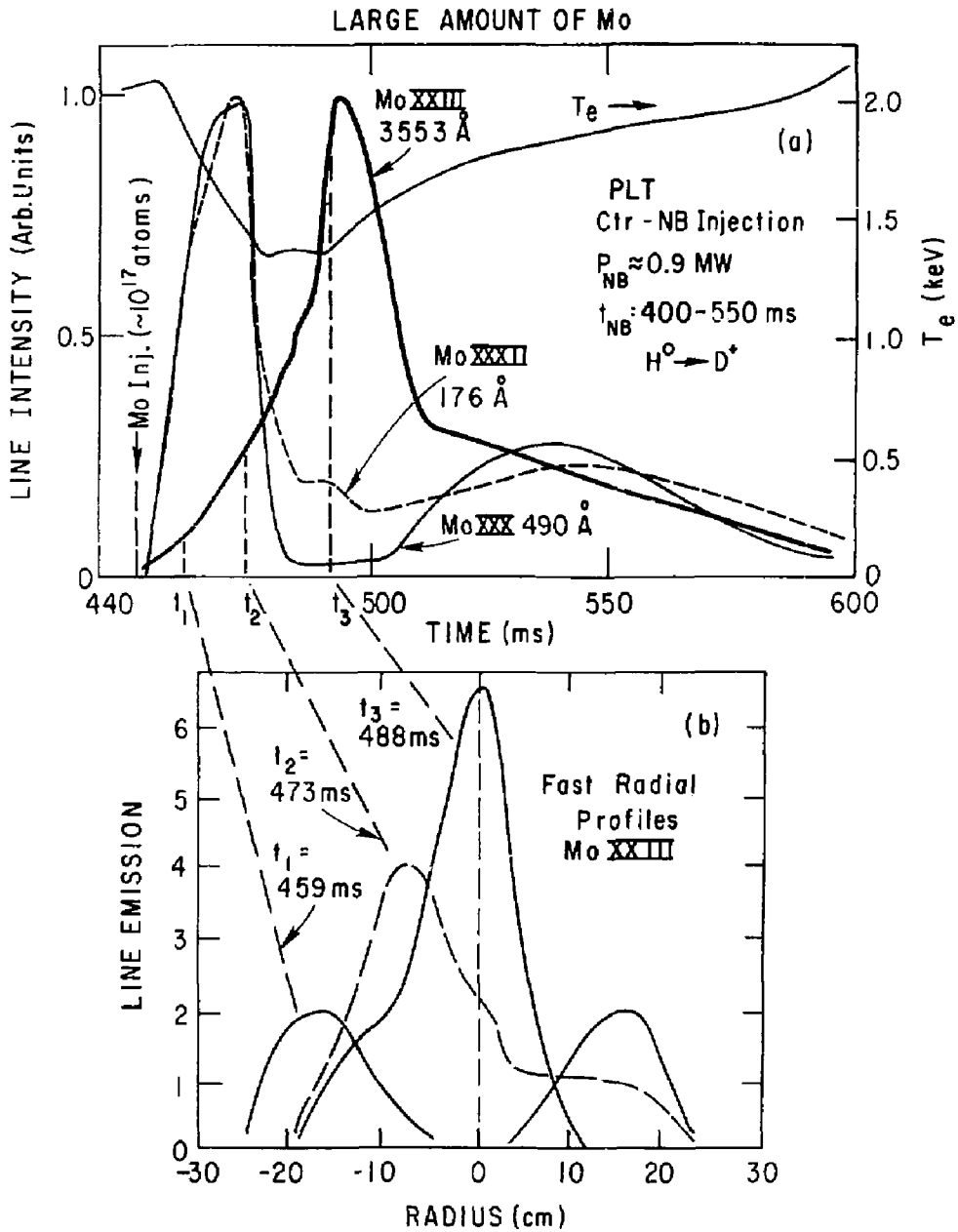

FIG. 12

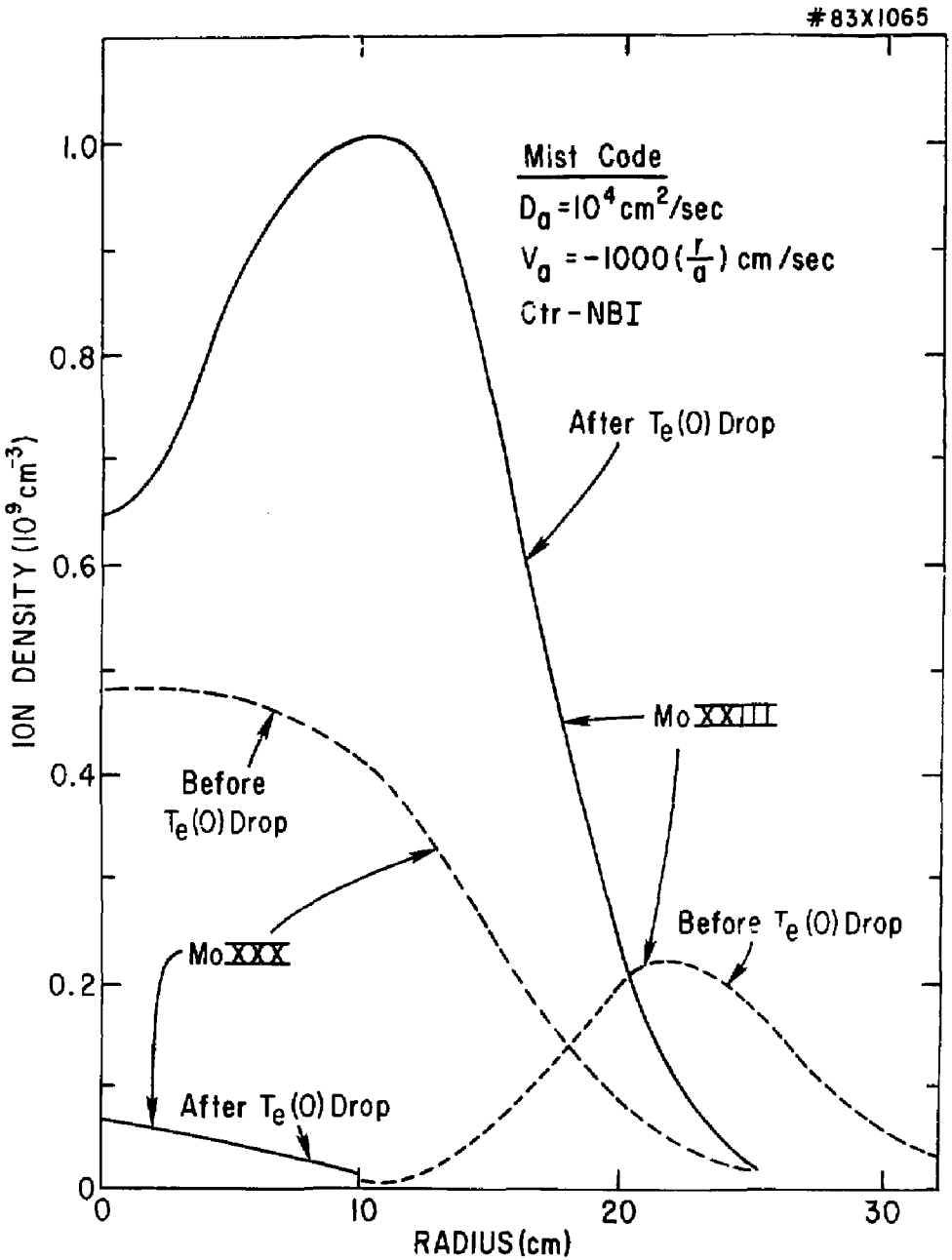
#83X1065
Mist Code
$D_a = 10^4 cm^2/sec$
$V_a = -1000(\frac{r}{a})$ cm/sec
Ctr-NBI
After $T_e(0)$ Drop
Mo XXIII
Before $T_e(0)$ Drop
Before $T_e(0)$ Drop
Mo XXX
After $T_e(0)$ Drop
ION DENSITY ($10^9 cm^{-3}$)
RADIUS (cm)
0
0.2
0.4
0.6
0.8
1.0
0
10
20
30

FIG. 13

83X0654

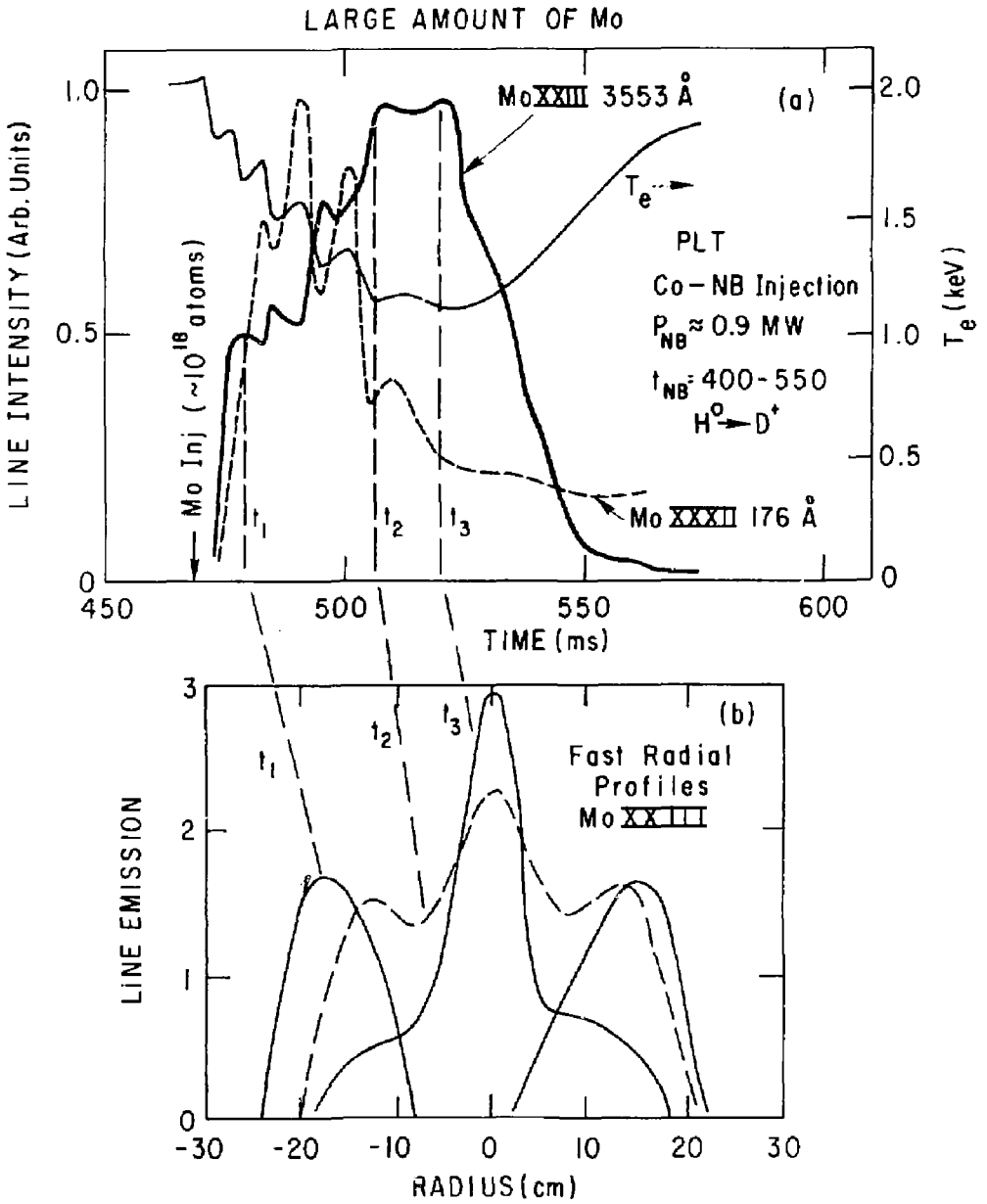

FIG. 14

EXTERNAL DISTRIBUTION IN ADDITION TO TIC UC-20

Plasma Res Lab, Austra Nat'l Univ, AUSTRALIA
Dr. Frank J. Paoloni, Univ of Wollongong, AUSTRALIA
Prof. I.R. Jones, Flinders Univ., AUSTRALIA
Prof. M.H. Brennan, Univ Sydney, AUSTRALIA
Prof. F. Cap, Inst Theo Phys, AUSTRIA
Prof. Frank Verheest, Inst theoretische, BELGIUM
Dr. D. Palumbo, Dg XII Fusion Prog, BELGIUM
Ecole Royale Militaire, Lab de Phys Plasmas, BELGIUM
Dr. P.H. Sakanaka, Univ Estadual, BRAZIL
Dr. C.R. James, Univ of Alberta, CANADA
Prof. J. Teichmann, Univ of Montreal, CANADA
Dr. H.M. Skarsgard, Univ of Saskatchewan, CANADA
Prof. S.R. Sreenivasan, University of Calgary, CANADA
Prof. Tudor W. Johnston, INRS-Energie, CANADA
Dr. Hannes Barnard, Univ British Columbia, CANADA
Dr. M.P. Bachynski, MPB Technologies, Inc., CANADA
Zhengwu Li, Sw Inst Physics, CHINA
Library, Tsing Hua University, CHINA
Librarian, Institute of Physics, CHINA
Inst Plasma Phys, Academia Sinica, CHINA
Dr. Peter Lukac, Komenskeho Univ, CZECHOSLOVAKIA
The Librarian, Culham Laboratory, ENGLAND
Prof. Schatzman, Observatoire de Nice, FRANCE
J. Radet, CEN-BP6, FRANCE
AM Dupas Library, AM Dupas Library, FRANCE
Dr. Tom Mual, Academy Bibliographic, HONG KONG
Preprint Library, Cent Res Inst Phys, HUNGARY
Dr. S.K. Trehan, Panjab University, INDIA
Dr. Indra, Mohan Lal Das, Banaras Hindu Univ, INDIA
Dr. L.K. Chavda, South Gujarat Univ, INDIA
Dr. R.K. Chhajlani, Var Ruchi Marg, INDIA
P. Kaw, Physical Research Lab, INDIA
Dr. Phillip Rosenau, Israel Inst Tech, ISRAEL
Prof. S. Cuperman, Tel Aviv University, ISRAEL
Prof. G. Rostagni, Univ Di Padova, ITALY
Librarian, Int'l Ctr Theo Phys, ITALY
Miss Clelia De Palo, Assoc EURATOM-CNEN, ITALY
Biblioteca, del CNR EURATOM, ITALY
Dr. H. Yamato, Toshiba Res & Dev JAPAN
Prof. M. Yoshikawa, JAERI, Tokai Res Est, JAPAN
Prof. T. Uchida, University of Tokyo, JAPAN
Research Info Center, Nagoya University, JAPAN
Prof. Kyoji Nishikawa, Univ of Hiroshima, JAPAN
Prof. Sigeru Mori, JAERI, JAPAN
Library, Kyoto University, JAPAN
Prof. Ichiro Kawakami, Nihon Univ, JAPAN
Prof. Satoshi Itoh, Kyushu University, JAPAN
Tech Info Division, Korea Atomic Energy, KOREA
Dr. R. England, Ciudad Universitaria, MEXICO
Bibliotheek, Fom-Inst Voor Plasma, NETHERLANDS
Prof. B.S. Liley, University of Waikato, NEW ZEALAND
Dr. Suresh C. Sharma, Univ of Calabar, NIGERIA
Prof. J.A.C. Cabral, Inst Superior Tech, PORTUGAL
Dr. Octavian Petrus, ALI CUZA University, ROMANIA
Prof. M.A. Hellberg, University of Natal, SO AFRICA
Dr. Johan de Villiers, Atomic Energy Bd, SO AFRICA
Fusion Div, Library, JEN, SPAIN
Prof. Hans Wilhelmson, Chalmers Univ Tech, SWEDEN
Dr. Lennart Stenflo, University of UMEA, SWEDEN
Library, Royal Inst Tech, SWEDEN
Dr. Erik T. Karlson, Uppsala Universitet, SWEDEN
Centre de Recherchesen, Ecole Polytech Fed, SWITZERLAND
Dr. W.L. Weise, Nat'l Bur Stand, USA
Dr. W.M. Stacey, Georg Inst Tech, USA
Dr. S.T. Wu, Univ Alabama, USA
Prof. Norman L. Oleson, Univ S Florida, USA
Dr. Benjamin Ma, Iowa State Univ, USA
Prof. Magne Kristiansen, Texas Tech Univ, USA
Dr. Raymond Askew, Auburn Univ, USA
Dr. V.T. Tolok, Kharkov Phys Tech Ins, USSR
Dr. D.D. Ryutov, Siberian Acad Sci, USSR
Dr. G.A. Eliseev, Kurchatov Institute, USSR
Dr. V.A. Glukhikh, Inst Electro-Physical, USSR
Institute Gen. Physics, USSR
Prof. T.J. Boyd, Univ College N Wales, WALES
Dr. K. Schindler, Ruhr Universitat, W. GERMANY
Nuclear Res Estab, Julich Ltd, W. GERMANY
Librarian, Max-Planck Institut, W. GERMANY
Dr. H.J. Kaeppler, University Stuttgart, W. GERMANY
Bibliothek, Inst Plasmaforschung, W. GERMANY